

Exact solution of the Faddeev-Volkov model

Vladimir V. Bazhanov, Vladimir V. Mangazeev, and Sergey M. Sergeev

*Department of Theoretical Physics,
Research School of Physical Sciences and Engineering,
Australian National University,
Canberra, ACT 0200, Australia.*

The Faddeev-Volkov model is an Ising-type lattice model with positive Boltzmann weights where the spin variables take continuous values on the real line. It serves as a lattice analog of the sinh-Gordon and Liouville models and intimately connected with the modular double of the quantum group $U_q(sl_2)$. The free energy of the model is exactly calculated in the thermodynamic limit. In the quasi-classical limit $c \rightarrow +\infty$ the model describes quantum fluctuations of discrete conformal transformations connected with the Thurston's discrete analogue of the Riemann mappings theorem. In the strongly-coupled limit $c \rightarrow 1$ the model turns into a discrete version of the $\mathcal{D} = 2$ Zamolodchikov's "fishing-net" model.

Faddeev and Volkov [1, 2, 3] obtained a very interesting solution of the star-triangle relation. There is only a few two-dimensional solvable lattice models [4] where the Yang-Baxter equation takes its distinguished "star-triangular" form. These models include the Ashkin-Teller [5], Kashiwara-Miwa [6] and chiral Potts [7] models (the latter also contains the Ising, self-dual Potts [8] and Fateev-Zamolodchikov [9] models as particular cases). All above models are also distinguished by a positivity of Boltzmann weights — the property that is naturally expected for physical applications, but rarely realized for generic solutions of the Yang-Baxter equation. Recently, we have observed [10] that the Faddeev-Volkov model [1, 2, 3] also possesses the positivity property. Apart from being an interesting model of statistical mechanics and quantum field theory in its own rights (it serves as a lattice version of the sinh-Gordon and Liouville models [11, 12]) this model has remarkable connections with discrete geometry. As shown in [10] it describes quantum fluctuations of circle patterns [13] and associated discrete conformal transformations connected with Thurston's discrete analogue of the Riemann mapping theorem [14].

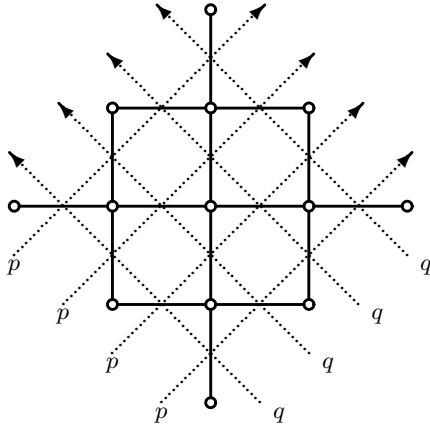


FIG. 1: The square lattice (solid lines) and its medial "rapidity" lattice (dashed lines).

Consider the square lattice, shown in Fig.1. Each site i of a lattice is assigned with a spin variable $\sigma_i \in \mathbb{R}$, taking *continuous real values*. Two spins a and b interact only if they are adjacent (connected with an edge of the lattice). Typical horizontal and vertical edges are shown in Fig.2. The corresponding Boltzmann weights are parametrized through the so-called "rapidity variables" p and q associated with the oriented dashed lines in Fig.1. In our case the weights depends only on the spin and rapidity differences $a - b$ and $p - q$, where a and b are the spins at the ends of the edge. We will denote them as $W_{p-q}(a - b)$ and $\overline{W}_{p-q}(a - b)$ for the horizontal and vertical edges, respectively. The partition function is defined as

$$Z = \int \prod_{(i,j)} W_{p-q}(\sigma_i - \sigma_j) \prod_{(k,l)} \overline{W}_{p-q}(\sigma_k - \sigma_l) \prod_i d\sigma_i. \quad (1)$$

where the first product is over all horizontal edges (i, j) and the second is over all vertical edges (k, l) . The integral is taken over all the interior spins; the boundary spins are kept fixed. The weights $W_{p-q}(a - b)$ and

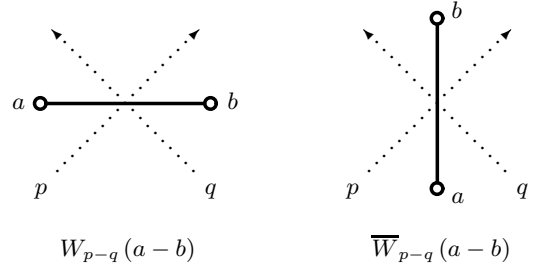


FIG. 2: Two types of Boltzmann weights.

$\overline{W}_{p-q}(a - b)$ are related with non-compact representations [15] of the modular double [16] of the quantum group $U_q(sl_2) \otimes U_{\tilde{q}}(sl_2)$, where $q = e^{i\pi b^2}$ and $\tilde{q} = e^{-i\pi/b^2}$. The modular parameter b is connected to the Liouville central charge $c_L = 1 + 6(b + b^{-1})^2$. It is convenient to define

$$\eta = \frac{1}{2}(b + b^{-1}), \quad \bar{q} = i \exp\left(\frac{i\pi(b - b^{-1})}{2(b + b^{-1})}\right). \quad (2)$$

The main physical regimes of the model

$$(i) \mathbf{b} > 0, \quad \text{and} \quad (ii) |\mathbf{b}| = 1, \quad \text{Im}(\mathbf{b}^2) > 0. \quad (3)$$

correspond to real values of η . For the regime (i) it is enough to consider the range $0 < \mathbf{b} \leq 1$ (due to the symmetry $\mathbf{b} \leftrightarrow \mathbf{b}^{-1}$).

Introduce the non-compact quantum dilogarithm [3],

$$\begin{aligned} \varphi(z) &= \exp\left(\frac{1}{4} \int_{\mathbb{R}+i0} \frac{e^{-2izw}}{\sinh(w\mathbf{b})\sinh(w/\mathbf{b})} \frac{dw}{w}\right) \\ &= \frac{(-\mathbf{q} e^{2\pi z \mathbf{b}}; \mathbf{q}^2)_\infty}{(-\tilde{\mathbf{q}} e^{2\pi z \mathbf{b}^{-1}}; \tilde{\mathbf{q}}^2)_\infty}, \end{aligned} \quad (4)$$

where $(x, \mathbf{q})_\infty = \prod_{k=0}^{\infty} (1 - \mathbf{q}^k x)$. The product representation above is valid for $\text{Im}(\mathbf{b}^2) > 0$.

The Boltzmann weights $W_\theta(s)$ and $\overline{W}_\theta(s)$ are defined as

$$W_\theta(s) = \frac{1}{F_\theta} e^{2\eta\theta s} \frac{\varphi(s + i\eta\theta/\pi)}{\varphi(s - i\eta\theta/\pi)}, \quad \overline{W}_\theta(s) = W_{\pi-\theta}(s), \quad (5)$$

where θ and s stand for the rapidity and spin differences, respectively. The normalization factor F_θ has the form

$$F_\theta = e^{i\eta^2\theta^2/\pi + i\pi(1-8\eta^2)/24} \Phi(2i\eta\theta/\pi). \quad (6)$$

where

$$\begin{aligned} \Phi(z) &= \exp\left(\frac{1}{8} \int_{\mathbb{R}+i0} \frac{e^{-2izw}}{\sinh(w\mathbf{b})\sinh(w/\mathbf{b})\cosh(2w\eta)} \frac{dw}{w}\right) \\ &= \frac{(\mathbf{q}^2 e^{2\pi z \mathbf{b}}; \mathbf{q}^4)_\infty}{(\tilde{\mathbf{q}}^2 e^{2\pi z \mathbf{b}^{-1}}; \tilde{\mathbf{q}}^4)_\infty} \frac{(-\tilde{\mathbf{q}} e^{\pi z/(2\eta)}; \tilde{\mathbf{q}}^2)_\infty}{(\tilde{\mathbf{q}} e^{\pi z/(2\eta)}; \tilde{\mathbf{q}}^2)_\infty} \end{aligned} \quad (7)$$

with $\tilde{\mathbf{q}}$ defined in (2). The main properties of $\varphi(z)$ and $\Phi(z)$ are discussed in [10].

When the parameter \mathbf{b} belongs to either of the regimes (3), the Boltzmann weights $W_\theta(s)$ and $\overline{W}_\theta(s)$ are real and positive for $0 < \theta < \pi$ and real s . They are even functions of the variable s and decay exponentially, $W_\theta(s) \simeq F_\theta^{-1} e^{-2\eta\theta|s|}$, when $s \rightarrow \pm\infty$. The weight $W_\theta(s)$, considered as a function of θ at fixed real s , is analytic and non-zero in the strip $0 < \text{Re} \theta < \pi$.

The weights W_θ and \overline{W}_θ satisfy several functional relations: the duality relation

$$\overline{W}_\theta(s) = \int_{\mathbb{R}} dx e^{2\pi i x s} W_\theta(x), \quad (8)$$

the inversion relations,

$$\begin{aligned} \lim_{\varepsilon \rightarrow 0^+} \int_{\mathbb{R}} dc \overline{W}_{it+\varepsilon}(a-c) \overline{W}_{-it+\varepsilon}(c-b) &= \delta(a-b), \\ W_\theta(a-b) W_{-\theta}(a-b) &= 1, \end{aligned} \quad (9)$$

where t is real, and the star-triangle relation, Fig.3:

$$\begin{aligned} \int_{\mathbb{R}} d\sigma \overline{W}_{q-r}(a-\sigma) W_{p-r}(c-\sigma) \overline{W}_{p-q}(\sigma-b) \\ = W_{p-q}(c-a) \overline{W}_{p-r}(a-b) W_{q-r}(c-b). \end{aligned} \quad (10)$$

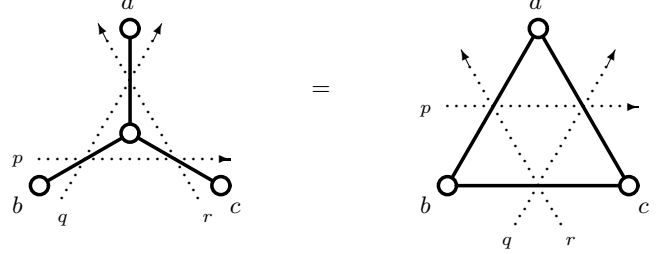


FIG. 3: Star-triangle relation.

We used the inversion relation method [17, 18, 19] to exactly calculate the partition function (1) in the thermodynamic limit. The result is included in the normalization of the Boltzmann weights, so that the free energy per edge,

$$\beta f_{edge} = - \lim_{N \rightarrow \infty} N^{-1} \log Z = 0, \quad (11)$$

vanishes when the number of edges, N , tends to infinity (provided the boundary spins are kept finite). The weights (5) attain their maximal values at $s = 0$. In the quasi-classical regime (i), $0 < \mathbf{b} < 1$, the value of the constant $W_{\frac{\pi}{2}}(0)$ slowly interpolates between the values

$$W_{\frac{\pi}{2}}(0) \Big|_{\mathbf{b}=0} = e^{\frac{G}{\pi}}, \quad W_{\frac{\pi}{2}}(s) \Big|_{\mathbf{b}=1} = \sqrt{2}, \quad (12)$$

where $G = 0.915965\dots$ is the Catalan's constant. The s -dependence of the two-spin interaction energy $E(s) = -\log W_{\frac{\pi}{2}}(s)$ is quadratic, $E(s) - E(0) \simeq s^2$, for small s and gradually becomes linear, $E(s) \simeq \pi\eta|s|$, for large s .

The parameter \mathbf{b}^2 plays the role of the Planck constant. The quasi-classical limit $\mathbf{b} \rightarrow 0$ (where the model reveals remarkable connections with the discrete geometry) was considered in [10]. It is worth mentioning some details here. When $\mathbf{b} \rightarrow 0$ the weight function $W_\theta(s)$ acquires a very narrow bell-shaped form and rapidly decays outside the small interval $|s| < \mathbf{b}/\theta$. The partition function (1) can be then calculated with saddle point method. It is convenient to define $\theta = p - q$ and use rescaled spin variables $\rho = \{\rho_1, \rho_2, \dots\}$, given by $\rho_i = 2\pi\mathbf{b}\sigma_i$. The leading asymptotics of (5) reads

$$W_\theta(\rho/2\pi\mathbf{b}) = e^{-A(\theta|\rho)/2\pi\mathbf{b}^2 + O(\mathbf{b}^0)}, \quad \mathbf{b} \rightarrow 0, \quad (13)$$

where the function

$$A(\theta|\rho) = \frac{1}{i} \int_0^\rho \log f_\theta(\xi) d\xi, \quad f_\theta(\xi) = \frac{1 + e^{\xi+i\theta}}{e^\xi + e^{i\theta}} \quad (14)$$

is simply related to the Euler dilogarithm. The stationary point of the integral (1) is determined by the classical equation of motion

$$f_\theta(\rho_W - \rho) f_{\pi-\theta}(\rho_N - \rho) f_\theta(\rho_E - \rho) f_{\pi-\theta}(\rho_S - \rho) = 1, \quad (15)$$

connecting five neighboring spins $\rho_W, \rho_N, \rho_E, \rho_S$ and ρ , arranged as in Fig.4 This non-linear difference equation

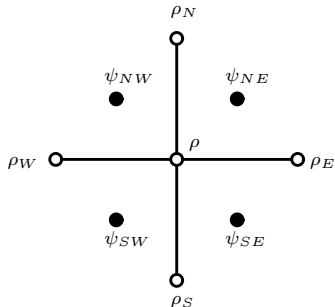


FIG. 4: Arrangement of the ρ - and ψ -variables around a four-edge star.

is a particular (square lattice) case of the ‘‘cross-ratio equations’’ [20, 21]. The latter can be viewed as discrete analogues of the Cauchy-Riemann conditions for analytic functions. In particular, Eq.(15) defines discrete conformal transformations [26] of the square lattice [20, 22], where the local dilatation factors $r_i = \exp(\rho_i)$ are determined by the rescaled spin variables ρ_i , solving (15).

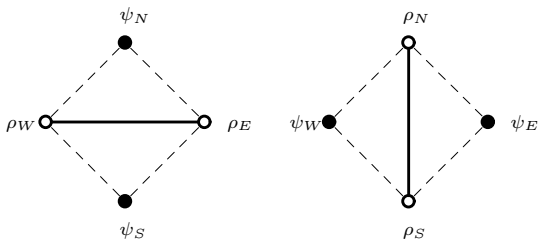


FIG. 5: Types of faces containing white and black sites.

The cross ratio equations (15) are closely related to the Hirota difference equation [23]. Place a purely imaginary variable ψ_i , $0 \leq \text{Im } \psi_i < 2\pi$, on every site i of the dual lattice. These sites are shown by black dots located in Figs. 4 and 5. Connect these new variables to the existing variables ρ_i by the following rules. Let ψ_N and ψ_S be the variables located above and below of a horizontal edge, as in Fig. 5. Then, we require that

$$e^{\psi_N - \psi_S} = \frac{e^{\rho_W} + e^{\rho_E + i\theta}}{e^{\rho_E} + e^{\rho_W + i\theta}}. \quad (16)$$

Similarly for a vertical edge,

$$e^{\psi_E - \psi_W} = \frac{e^{\rho_N} + e^{\rho_S + i\theta^*}}{e^{\rho_S} + e^{\rho_N + i\theta^*}} \Rightarrow e^{\rho_N - \rho_S} = \frac{e^{\psi_W} + e^{\psi_E + i\theta}}{e^{\psi_E} + e^{\psi_W + i\theta}}, \quad (17)$$

where $\theta^* = \pi - \theta$. The consistency of these definitions across the lattice is provided by (15). Note that the second form of (17) is identical to (16) upon interchanging all ψ - and ρ -variables. Therefore it is natural to associate this universal equation with every face of the ‘‘double’’ lattice consisting of all white and black sites (its faces are shown in Fig. 5). This is the famous Hirota equation introduced in [23].

Thus, in the quasi-classical limit $\mathbf{b} \rightarrow 0$ the stationary points of the integral (1) defines discrete analogs of conformal transformations. At finite values of \mathbf{b} the model describes quantum fluctuations of these transformations. Given that the spins ρ_i define the local dilatation factors the Faddeev-Volkov model describes a *quantum discrete dilaton*. The continuous quantum field theory with the conformal symmetry [24] has remarkable applications in physics and mathematics. It would be interesting to understand which aspects of the continuous conformal field theory can be transferred to the discrete case.

For the ‘‘strongly coupled’’ regime (ii), when the parameter \mathbf{b} is on the unit circle $|\mathbf{b}| = 1$, the function $W_{\frac{\pi}{2}}(s)$ still has its absolute maximum at $s = 0$ but starts to develop additional side maxima at integer points when $\arg(\mathbf{b})$ approaches the value $\pi/2$. The first pair of such

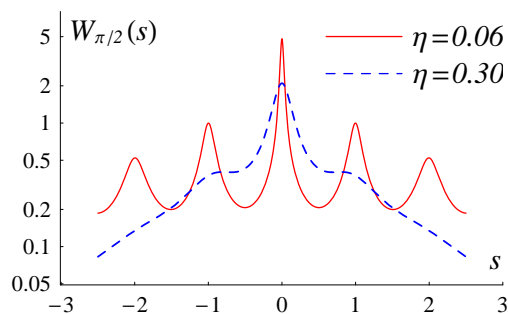


FIG. 6: The function $W_{\pi/2}(s)$ for $\eta = 0.30$ and 0.06 .

side maxima at $s = \pm 1$ appears when $\eta \simeq \cos(2\pi/5) \simeq 0.309$, see Fig. 6. For $\eta = 0$ the function $W_{\frac{\pi}{2}}(s)$ turns into a superposition of δ -function like peaks at $s \in \mathbb{Z}$. In particular, the height of the central maximum diverges as

$$W_{\frac{\pi}{2}}(0) \simeq (2\pi\eta)^{-1/2} \Gamma(\frac{1}{4})/\Gamma(\frac{3}{4}) + O(\eta^{1/2}), \quad \eta \rightarrow 0. \quad (18)$$

A more careful limiting procedure capturing a fine structure of these sharp peaks requires a redefinition of the spin variables. Using the asymptotics

$$\varphi(n + x\eta) \simeq e^{-i\pi/12} (4\pi\eta)^{ix} \Gamma(\frac{1-n+ix}{2})/\Gamma(\frac{1-n-ix}{2}),$$

$$\Phi(2x\eta) \simeq e^{-i\pi/24} (8\pi\eta)^{ix} \Gamma(\frac{1+ix}{2})/\Gamma(\frac{1-ix}{2}), \quad (19)$$

where $\eta \rightarrow 0$, $n \in \mathbb{Z}$ and $|x| \ll \eta^{-1}$, it is easy to see that

$$W_\theta(n + x\eta) \simeq \eta^{-\theta/\pi} V_\theta(n, x), \quad \eta \rightarrow 0 \quad (20)$$

where the function,

$$V_\theta(n, x) = \frac{1}{(2\pi)^{\frac{\theta}{\pi}}} \frac{\Gamma(\frac{1+\theta/\pi}{2})\Gamma(\frac{1-n-\theta/\pi+ix}{2})\Gamma(\frac{1-n-\theta/\pi-ix}{2})}{\Gamma(\frac{1-\theta/\pi}{2})\Gamma(\frac{1-n+\theta/\pi+ix}{2})\Gamma(\frac{1-n+\theta/\pi-ix}{2})} \quad (21)$$

is real and positive for $n \in \mathbb{Z}$ and $x \in \mathbb{R}$. This function defines Boltzmann weights for a new model where

The star-triangle relation for $V_\theta(n, x)$ simply follows from (10),

$$\begin{aligned} \sum_{n_0 \in \mathbb{Z}} \int_{\mathbb{R}} dx_0 V_{\theta_1}(n_1 - n_0; x_1 - x_0) V_{\theta_2}(n_2 - n_0; x_2 - x_0) V_{\theta_3}(n_3 - n_0; x_3 - x_0) \\ = V_{\pi-\theta_1}(n_2 - n_3; x_2 - x_3) V_{\pi-\theta_2}(n_1 - n_3; x_1 - x_3) V_{\pi-\theta_3}(n_1 - n_2; x_1 - x_2), \end{aligned} \quad (22)$$

where $\theta_1 + \theta_2 + \theta_3 = 2\pi$. Similarly, the inversion relations (9) imply

$$\lim_{\varepsilon \rightarrow 0^+} \sum_{n_2 \in \mathbb{Z}} \int_{\mathbb{R}} dx_2 V_{\pi+\varepsilon}(n_1 - n_2; x_1 - x_2) V_{\pi-\varepsilon}(n_2 - n_3; x_2 - x_3) = \delta_{n_1, n_3} \delta(x_1 - x_3), \quad V_\theta(n, x) V_{-\theta}(n, x) = 1 \quad (23)$$

The Boltzmann weight $V_\theta(n; x)$ is an even function of n and x ; it satisfies the following initial conditions

$$V_\pi(n; x) = \delta_{n,0} \delta(x), \quad V_0(n; x) = 1. \quad (24)$$

Note that its asymptotics when $n, x \rightarrow \pm\infty$,

$$V_\theta(n; x) \simeq \left(\frac{2}{\pi}\right)^{\theta/\pi} \frac{\Gamma(\frac{1+\theta/\pi}{2})}{\Gamma(\frac{1-\theta/\pi}{2})} |n^2 + x^2|^{-\theta/\pi}, \quad (25)$$

coincides with the *normalized* Boltzmann weight of the $\mathcal{D} = 2$ Zamolodchikov's "fishing-net" model [25] (except that the variable n in our case is discrete). It follows from (11) that with this normalization the specific free energy of the "fishing-net" model vanishes in the thermodynamic limit in complete agreement with [25].

each lattice site i is assigned with a pair of fluctuating variables (n_i, x_i) , where $n_i \in \mathbb{Z}$ take integer values and $x_i \in \mathbb{R}$ take continuous values on the real line. Its partition function is defined by (1) where $W_\theta(\sigma_i - \sigma_j)$ replaced by $V_\theta(n_i - n_j, x_i - x_j)$ (and similarly for \bar{W}) and every integral over σ_i is replaced by a sum over n_i and an integral over x_i , namely $\int d\sigma_i \rightarrow \sum_{n_i \in \mathbb{Z}} \int dx_i$.

-
- [1] Volkov, A. Y. Quantum Volterra model. Phys. Lett. A **167** (1992) 345–355.
 - [2] Faddeev, L. and Volkov, A. Y. Abelian current algebra and the Virasoro algebra on the lattice. Phys. Lett. B **315** (1993) 311–318.
 - [3] Faddeev, L. Currentlike variables in massive and massless integrable models. In *Quantum groups and their applications in physics (Varenna, 1994)*, volume 127 of *Proc. Internat. School Phys. Enrico Fermi*, pages 117–135, Amsterdam, 1996. IOS.
 - [4] Baxter, R. J. *Exactly Solved Models in Statistical Mechanics*. Academic Press Inc., London, 1982.
 - [5] Ashkin, J. and Teller, E. Statistics of Two-Dimensional Lattices with Four Components. Physical Review **64** (1943) 178–184.
 - [6] Kashiwara, M. and Miwa, T. A class of elliptic solutions to the star-triangle relation. Nuclear Physics B **275** (1986) 121–134.
 - [7] Baxter, R. J., Perk, J. H. H., and Au-Yang, H. New solutions of the star triangle relations for the chiral Potts model. Phys. Lett. **A128** (1988) 138–142.
 - [8] Potts, R. B. Some generalized order-disorder transformations. Proceedings of the Cambridge Philosophical Society **48** (1952) 106–109.
 - [9] Fateev, V. A. and Zamolodchikov, A. B. Self-dual solutions of the star-triangle relations in Z_N -models. Phys. Lett. A **92** (1982) 37–39.
 - [10] Bazhanov, V. V., Mangazeev, V. V., and Sergeev, S. M. Faddeev-Volkov model solution of the Yang-Baxter equation and discrete conformal symmetry. arXiv:hep-th/0703041, in press Nucl. Phys. B., 2007.
 - [11] Faddeev, L. D., Kashaev, R. M., and Volkov, A. Y. Strongly coupled quantum discrete Liouville theory. I. Algebraic approach and duality. Commun. Math. Phys. **219** (2001) 199–219.
 - [12] Bytsko, A. G. and Teschner, J. Quantization of models with non-compact quantum group symmetry: Modular XXZ magnet and lattice sinh-Gordon model. J. Phys. **A39** (2006) 12927–12981.
 - [13] Bobenko, A. I. and Springborn, B. A. Variational principles for circle patterns and Koebe's theorem. Trans. Amer. Math. Soc. **365** (2004) 659689.
 - [14] Stephenson, K. Circle packing: a mathematical tale. Notices Amer. Math. Soc. **50** (2003) 13761388.
 - [15] Ponsot, B. and Teschner, J. Liouville bootstrap via harmonic analysis on a noncompact quantum group, 1999. hep-th/9911110.
 - [16] Faddeev, L. Modular double of a quantum group. In *Conférence Moshé Flato 1999, Vol. I (Dijon)*, volume 21 of *Math. Phys. Stud.*, pages 149–156, Dordrecht, 2000. Kluwer Acad. Publ.
 - [17] Stroganov, Y. G. A new calculation method for partition functions in some lattice models. Phys. Lett. A **74** (1979) 116–118.
 - [18] Zamolodchikov, A. B. Z_4 -symmetric factorized S -matrix in two space-time dimensions. Comm. Math. Phys. **69**

- (1979) 165–178.
- [19] Baxter, R. J. The inversion relation method for some two-dimensional exactly solved models in lattice statistics. *J. Statist. Phys.* **28** (1982) 1–41.
- [20] Bobenko, A. I. and Suris, Y. B. Integrable systems on quad-graphs. *Int. Math. Res. Not.* (2002) 573–611.
- [21] Nijhoff, F. and Capel, H. The discrete Korteweg-de Vries equation. *Acta Appl. Math.* **39** (1995) 133–158. KdV '95 (Amsterdam, 1995).
- [22] Schramm, O. Circle patterns with the combinatorics of the square grid. *Duke Math. J.* **86** (1997) 347389.
- [23] Hirota, R. Nonlinear partial difference equations. III. Discrete sine-Gordon equation. *J. Phys. Soc. Japan* **43** (1977) 2079–2086.
- [24] Belavin, A. A., Polyakov, A. M., and Zamolodchikov, A. B. Infinite conformal symmetry in two-dimensional quantum field theory. *Nuclear Phys. B* **241** (1984) 333–380.
- [25] Zamolodchikov, A. B. “Fishing-net” diagrams as a completely integrable system. *Phys. Lett. B* **97** (1980) 63–66. Note that there is a misprint in Eq.(18) of this paper. The RHS of that equation defines e^f (rather than e^{-f}), where f is the specific free energy per edge of the lattice.
- [26] These transformations are nicely visualized by the circle patterns with prescribed intersection angles [13] The (rescaled) spin variables, solving (15), define the radii $r_i = e^{\rho_i}$ of the circles, while the rapidity variable θ defines the circle intersection angles, see [10] for more details.